PROTEINS
STRUCTURE ■ FUNCTION ■ BIOINFORMATICS

Solution structure and interface-driven self-assembly of NC2, a new member of the Class II hydrophobin proteins

Qin Ren,[1] Ann H. Kwan,[2]* and Margaret Sunde[1]*

[1] Discipline of Pharmacology, School of Medical Sciences, University of Sydney, Sydney, New South Wales, 2006, Australia

[2] School of Molecular Bioscience, University of Sydney, Sydney, New South Wales, 2006, Australia

ABSTRACT

Hydrophobins are fungal proteins that self-assemble spontaneously to form amphipathic monolayers at hydrophobic:hydrophilic interfaces. Hydrophobin assemblies facilitate fungal transitions between wet and dry environments and interactions with plant and animal hosts. NC2 is a previously uncharacterized hydrophobin from *Neurospora crassa*. It is a highly surface active protein and is able to form protein layers on a water:air interface that stabilize air bubbles. On a hydrophobic substrate, NC2 forms layers consisting of an ordered network of protein molecules, which dramatically decrease the water contact angle. The solution structure and dynamics of NC2 have been determined using nuclear magnetic resonance spectroscopy. The structure of this protein displays the same core fold as observed in other hydrophobin structures determined to date, including the Class II hydrophobins HFBI and HFBII from *Trichoderma reesei*, but certain features illuminate the structural differences between Classes I and II hydrophobins and also highlight the variations between structures of Class II hydrophobin family members. The unique properties of hydrophobins have attracted much attention for biotechnology applications. The insights obtained through determining the structure, biophysical properties and assembly characteristics of NC2 will facilitate the development of hydrophobin-based applications.

Proteins 2014; 82:990–1003.

Key words: self-assembly; amphipathic; monolayer; hydrophobins; interface.

INTRODUCTION

Hydrophobins are a group of small proteins that are unique to filamentous fungi. Fungi secrete hydrophobins in a soluble form and the proteins self-assemble at hydrophobic:hydrophilic interfaces (HHIs) into amphipathic monolayers that are composed of highly ordered structures. Hydrophobin assemblies play many important roles in fungal biology, including reducing the surface tension of the growth medium to allow aerial hyphae to break through the air:liquid interface,[1] coating aerial structures and spores to render them hydrophobic and resistant to wetting,[2] and lining gas-exchange surfaces to prevent water logging.[3–7] They have also been shown to be of importance in pathogen:host interactions in plants[8] as well as in human infections.[9] Hydrophobins are considered to be one of the most surface-active molecules known. Their amphipathic nature is responsible for the ability of hydrophobins to lower the surface tension of a solution and change the wettability of a solid surface. It has also been demonstrated that hydrophobins can solubilize hydrophobic particles in aqueous solutions and stabilize emulsions. These unique proteins are currently being applied in many different areas of biotechnology, including development of biocompatible nanodevices and drug delivery.[10–12]

Additional Supporting Information may be found in the online version of this article.

Abbreviations: AFM, atomic force microscopy; FTIR, Fourier-transform infrared; HHI, hydrophobic:hydrophilic interface; NMR, nuclear magnetic resonance; TFA, trifluoroacetic acid; ThT, thioflavin T; Ni-NTA, nickel nitrilotriacetic acid; His6, hexa-histidine; Ub, ubiquitin; MS, mass spectrometry; RP-HPLC, reverse-phase high performance liquid chromatography

Grant sponsor: Australian Research Council; Grant numbers: DP0879121, DP1093949; Grant sponsor: National Health and Medical Research Council RD Wright Career Development Fellowship (to M.S.).

*Correspondence to: Ann H. Kwan, G08 - Molecular Bioscience Building, University of Sydney, Sydney, NSW, 2006, Australia. E-mail: ann.kwan@sydney.edu.au (or) Margaret Sunde, D06 Blackburn Building, University of Sydney, Sydney, NSW, 2006, Australia. E-mail: margaret.sunde@sydney.edu.au

Received 30 June 2013; Revised 20 October 2013; Accepted 29 October 2013
Published online 12 November 2013 in Wiley Online Library (wileyonlinelibrary.com). DOI: 10.1002/prot.24473

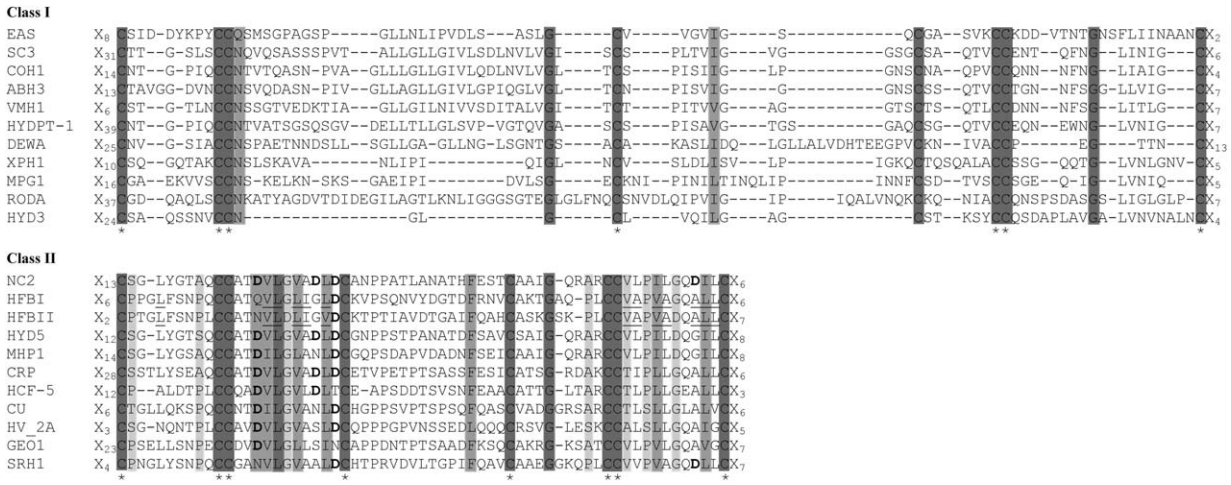

Figure 1

Sequence alignment of hydrophobin proteins. Only the amino acids between the first cysteine and the last cysteine residues are shown due to the large sequence variation at the protein termini. The numbers of residues that are present before the first cysteine or after the eighth cysteine are indicated as X_n, where n is the number of the residues. Cysteine residues are indicated with asterisks. Conserved residues are colored with a dark background and the degree of shading corresponds to the level of conservation. Residues that form the hydrophobic patch in the HFBI and HFBII structures are underlined. Aspartic acid residues forming the negatively charged area in NC2, and conserved in other Class II hydrophobins, are shown in bold. Proteins used in the alignments are EAS from *N. crassa* (Q04571), SC3 from *S. commune* (P16933), COH1 from *C. cinerea* (CAA71652), ABH3 from *A. bisporus* (CAA74939), VMH1 from *P. ostreatus* (CAB41405), HYDPT-1 from *P. tinctorius* (P52748), DewA from *A. nidulans* (P52750), XPH1 from *X. parietina* (CAC43386), MPG1 from *M. grisea* (P52751), RODA from *A. fumigatus* (AAB60712), HYD3 from *G. moniliformis* (AAO16869), NC2 from *N. crassa* (XP_959282), HFB1 from *T. reesei* (CAA92208), HFBII from *T. reesei* (CAA72636), HYD5 from *G. moniliformis* (AAN76355) MHP1 from *M. grisea* (AAD18059), CRP from *C. parasitica* (AAA19638), HCF-5 from *P. fulva* (CAC27408), CU from *O. ulmi* (Q06153), HV_2A from *T. virens* (EU053461), GEO1 from *G. pallida* (AFO38193), and SRH1 from *T. harzianum* (CAA72539).

The sequences of hydrophobins are relatively low in homology but are characterized by the presence of eight completely conserved cysteine residues. Hydrophobins can be further grouped into two classes according to the distribution of the hydrophobic residues along the sequence (Fig. 1).[13] Class II hydrophobins are generally much more conserved in both the amino acid composition and the length of the intervening segments between the cysteine residues, and they have a compact three-dimensional structure.[14–16] On the other hand, Class I hydrophobins are more varied in sequence, especially in the length and the amino acid composition of the segment between the third and the fourth cysteine residues, and their structures display a variety of secondary structural elements and some conformational flexibility around the hydrophobin core.[12] Monolayers formed by the two classes are both amphipathic but have distinctive properties. Class I monolayers are considered to be functional amyloids as they are composed of rod-like substructures known as rodlets which have an underlying cross-β amyloid structure. Hydrophobin rodlets are extremely stable and can only be depolymerized by treatment with concentrated strong acids such as trifluoroacetic acid and formic acid. Monolayers formed by Class II hydrophobin proteins do not have the amyloid-like substructure and they are much less stable; for example, they can be dissociated by treatment with ethanol and hot SDS.

A thorough understanding of these unique proteins, and their self-assembly mechanism, is crucial for understanding the role of hydrophobins in fungal biology and pathogen:host interactions as well as for developing novel hydrophobin-based biotechnology. We have therefore investigated the properties and structure of a second hydrophobin from *N. crassa*. The *N. crassa* genome encodes two hydrophobin proteins, one of which is the Class I hydrophobin EAS. The other is a putative Class II hydrophobin that we have termed NC2 for *N. crassa* hydrophobin Class II (NCU08192).[17] *NC2* gene expression has been shown to be upregulated when either of the photoreceptors WC-1 or WC-2 is deleted and increased cellulase activity in an *NC2* knockout mutant suggests that this protein might be involved in plant host response or interaction with the environment, however the function of the protein has not yet been clearly identified.[18] The full-length protein sequence includes what is predicted by SignalP 4.0[19] to be an N-terminal signal peptide for secretion, followed by a polypeptide chain of 80 amino acids, resulting in a predicted mature secreted protein with a size of 8.9 kDa. Despite the generally high sequence homology amongst Class II members, NC2 shares only 39% sequence identity with the well-studied Class II hydrophobin HFBII.

Contact angle measurements indicate that NC2 is highly surface active, and NC2 is able to stabilize air

bubbles in solution. In addition, NC2 forms monolayers on a hydrophobic surface that have a striking morphology and which are able to reduce the wettability of the surface. These properties are likely to underpin the biological role of this Class II hydrophobin in *N. crassa*. The self-assembly of NC2 is not accompanied by a significant conformational change and the NC2 monolayers are completely disrupted by treatment with detergent and hot alcohol, consistent with the expected character of Class II hydrophobin monolayers. The solution structure of NC2, determined by nuclear magnetic resonance (NMR) spectroscopy, reveals an open half β-barrel as the hydrophobin core. Analysis of backbone dynamics indicates that the two loop regions are slightly more mobile than the rest of the protein backbone and the N-terminus is highly flexible. This study points to the key differences between the Classes I and II hydrophobins likely to be responsible for the unique character of the two types of hydrophobin assembly that are utilized by filamentous fungi.

MATERIALS AND METHODS

Materials

All reagents and chemicals were purchased from Sigma-Aldrich, Astral Scientific, Amyl Media, or Ajax Finechem, apart from chromatography-grade methanol, which was purchased from Burdick & Jackson.

Production of NC2 protein

The synthetic gene of NC2 was subcloned into the pHUE expression vector, and the His_6-Ub-NC2 protein was expressed in *E. coli* Rosetta™ 2.DE3 cells at 37°C either in rich media or in minimal media using $^{15}NH_4Cl$ and ^{13}C-glucose as the sole nitrogen and carbon source, respectively. NC2 was purified under denaturing conditions as described by Kwan *et al.*[20] However, as NC2 was mostly found in the soluble fraction of the cell lysate, the whole cell pellets were lysed in the buffer containing 6*M* guanidine hydrochloride and 4.8 m*M* β-mercaptoethanol, and the fusion protein was extracted from the solubilized fraction using Ni-NTA agarose (Qiagen, Hilden, Germany). The correct molecular weight of purified NC2 was confirmed by mass spectrometry and 1D ^1H NMR spectroscopy indicated that the refolding process had resulted in a homogeneous preparation of a well-structured protein.

Size-exclusion chromatography and multiangle laser light scattering

Lyophilized protein was dissolved in 50 m*M* phosphate buffer (pH 7.0) containing 150 m*M* NaCl to final concentrations of 1, 2, 3, 4, and 5 mg/mL. Samples were analyzed on a Superdex 75 10/300 GL column (Amersham Biosciences) attached to an ÄKTA FPLC (Amersham Pharmacia Biotech) using a flow rate of 0.5 mL/min. Laser light scattering was detected with a Mini-DAWN light scattering detector (Wyatt Technology) and the refractive index of the eluant was measured using a Wyatt Optilab DSP refractometer (Wyatt Technology). The molecular weight of the species eluting as the major detected protein peak was calculated using the ASTRA software (Wyatt Technology).

Contact angle measurement

Protein solution drops (20 μL) containing 100 μg/mL of NC2 in Milli-Q® water were incubated on OTS-coated silicon wafers at room temperature for 30 min. The bulk protein solution was carefully removed after incubation, and the surface was left to dry in air. Water drops (10 μL) were dispensed at the centre of the protein-coated area to measure the water contact angle. The drop shape was analyzed using a Kruss DSA 10MK2 analyser (KRUSS, Hamburg, Germany) and accompanying software. Values given are the average from three drops.

Thioflavin T-binding assay

Lyophilized proteins were dissolved in buffer containing 50 m*M* Tris-HCl (pH 8.0), 40 μ*M* ThT, to a final protein concentration of 4 μ*M* for $EAS_{\Delta 15}$, and 3 μ*M* for NC2. Samples were prepared in 2-mL Wheaton glass vials, and vortexed with a Labnet VX100 Vortex Mixer at 3000 rpm. Samples were excited at 435 nm, and fluorescence was recorded from 450 to 600 nm using excitation and emission slit widths set to 10 nm on a Varian Cary Eclipse fluorescence spectrophotometer (Varian, Santa Clara, CA).

Fourier-transform infrared spectroscopy

Assembled NC2 was prepared by dissolving lyophilized NC2 in Milli-Q® water to a concentration of 50 μg/mL and then vortexing with a Labnet VX100 Vortex Mixer (Labnet International, Edison, NJ) at 3000 rpm at RT for 30 min, before lyophilization. Monomer samples were lyophilized soluble NC2 after purification by RP-HPLC. The Fourier-transform infrared (FTIR) spectra of assembled and monomeric NC2 were collected as described.[33]

Atomic force microscopy (AFM)

A 50-μL droplet of NC2 solution (5 μg/mL) was placed on a freshly cleaved HOPG (SPI, Holgate Scientific) surface, and allowed to dry in air at RT. The coated area was washed in a stream of running Milli-Q® water for 1 min, and then air-dried before analyzing with AFM. The morphology of the prepared HOPG surface

was characterized at ambient atmosphere, using a Multimode Nanoscope® III atomic force microscopy (Veeco, Santa Barbara, CA) operated in tapping mode. The AFM probes used were silicon scanning probes with a tip radius < 10 nm, and the force constant was 40 N/m and resonant frequency 300 kHz (Tap300AI-G, BudgetSensors™). Analysis of AFM images was performed with the Gwyddion software (version 2.30, http://gwyddion.net). To investigate the effect of different conditions, NC2 coated surfaces were prepared as above, and then incubated in respective conditions for 5 min. Bulk solution was wicked off by contact with a KimWipe, and then the surface was rinsed in running Milli-Q® water for 7 min, and then allowed to dry in air.

NMR spectroscopy

Samples containing either ^{15}N-labeled or ^{15}N^{13}C-labeled NC2 were prepared in 20 m*M* sodium phosphate buffer at pH 6.0 in 10 or 100% D_2O and 50 μ*M* DSS to final protein concentrations of 300–350 μ*M*. Spectra were acquired at 283 K on a Bruker Avance III 800 MHz spectrometer, which was equipped with a 5-mm triple resonance TCI cryoprobe (Bruker, Karlsruhe, Germany). To obtain the highest quality NMR spectra for structure determination and to investigate sample stability, ^{15}N-HSQC spectra were collected at pH 6.0 and 7.0 over a temperature range of 5°C to 25°C. No major changes in the peak positions or intensities were observed, suggesting the protein conformation remains the same under all the tested conditions (data not shown). The chemical shift assignment and solution structure of NC2 was determined at pH 6.0 and 10°C. Backbone and side chain assignments were made using the following experiments: HNCACB, CBCAcoNH, CCcoNH-TOCSY, HNCO, HNcaCO, HBHAcoNH, hCCH-TOCSY, HcCH-TOCSY, Hcc(co)NH-TOCSY.

During assignment, a second set of chemical shifts was identified for Leu68–Asp71, and Ala78–Leu80. The presence of two conformations for these regions could be due to the isomerization of the nearby proline residues (Pro66 and Pro77). However, only a single set of resonances could be identified for each of the seven proline residues in NC2, and all of these are in the *trans* conformation as judged by the chemical shifts of $^{13}C^{\beta}$ and $^{13}C^{\gamma}$ atoms.[21] Thr20 was also assigned with a second set of chemical shifts, and the reason for this is unclear. Generally, the second set of peaks is significantly weaker than the first set, and likely arose from the presence of a minor conformer. The assignment of ^{15}N and $^{1}H_N$ of Ala44 could not be made due to the absence of signal. In total, ~96% of backbone and ~90% of side chain atoms were assigned.

Unusual chemical shifts, defined as those lying outside two standard deviations from the average values reported in the BMRB database, were observed for $^{13}C^{\beta}$ of Gln22 (35.9 ppm), $^{13}C^{\gamma 2}$ of Thr26 (17.4 ppm), $^{15}N^{\epsilon}$ of Gln58 (105.2 ppm), and $^{1}H^{\beta}$ of Ala60 (−0.35 ppm). These are likely to be due to structural constraints imposed by the neighboring disulfide bonds. The chemical shift of $^{1}H_{\alpha}$ of Asn45 (2.5 ppm) is also found to be unusual, which may be explained by the close proximity of the nearby hydroxyl group of Tyr11. The distance of $^{1}H_{\alpha}$ of Asn45 to the phenolic hydroxyl of Tyr11 is less than 4 Å in 7 of the 20 lowest energy structures, but the side-chain orientation of Tyr11 is not very well defined.

All spectra were analyzed, and peaks picked manually, in CCPNmr Analysis 2.1.5.[22] ^{15}N-NOESY and ^{13}C-NOESY spectra were used as input into ARIA 2.3.1[23] implemented in CNS 1.2[24] together with the dihedral restraints derived from NMR data by DANGLE,[25] and four disulfide bond restraints. The disulfide bond connectivity was assumed to be the same as in all other hydrophobin structures that have been determined to date and this agreed well with the NOE-derived distance restraints. The calculation protocol comprised eight cycles of 20 structures each and a final cycle of 500 structures. Manually assigned NOEs were included in iteration zero as soft restraints. The cut-off value for an ambiguous assignment was reduced from 1.0 for the first iteration to 0.80 in iteration 8. A total of 1517 unambiguous and 69 ambiguous restraints were identified by ARIA, and these restraints were checked and corrected manually where necessary. The 20 conformers with the lowest value of E_{tot} were visualized and analyzed using MOLMOL[26] and PROCHECK-NMR[27] and the structural statistics for the ensembles are shown in Table I.

^{15}N T_1 (with T_1 relaxation delays of 0.005, 0.012, 0.06, 0.1, 0.15, 0.3, 0.6, 0.8, 1, 1.4, 1.5, and 2 s) and T_2 (with T_2 relaxation delays of 0.016, 0.032, 0.048, 0.064, 0.08, 0.096, 0.128, 0.16, 0.208, 0.224, 0.24, and 0.256 s) relaxation time constants, along with ^{15}N-^{1}H heteronuclear NOEs were measured using standard Bruker pulse programs. Peak heights were used and T_1 and T_2 data fitted to two-parameter exponentials using the relaxation module in CCPNmr Analysis 2.1.5.[22]

Accession numbers

Chemical shifts for NC2 were deposited in the BMRB under the accession code 18351 and the structure coordinates and NMR restraints were deposited in the PDB under the PDB ID 4aog.

RESULTS AND DISCUSSION

NC2 is highly surface active and assembles at air:water interfaces

Other Class II hydrophobins, HFBI and HFBII from *Trichoderma reesei*, have been found to form tetramers at 10 mg/mL, and to probably undergo monomer:dimer exchange at low concentrations.[28–30] To test whether

Table I
Structural Statistics for 20 Lowest Energy Models of NC2 Solution Structure

NMR restraints	
Total NOE restraints	1586
Total unambiguous restraints	1517
Intraresidues	690
Sequential	409
Short range (2–3 residues)	135
Medium range (4–5 residues)	39
Long range (>5 residues)	244
Total ambiguous restraints	69
Dihedral angle restraints	132
Disulfide bond restraints	4
Structure statistics	
PROCHECK statistics (residues 11–80)	
Residues in most favored regions	72.20%
Residues in allowed regions	26.30%
Residues in generously allowed regions	1.50%
Residues in disallowed regions	0.10%
Deviations from idealized geometry	
Bond lengths (Å)	0.003 ± 0.0001
Bond angles (°)	0.468 ± 0.042
Atomic RMSD (residues 11–80) (Å)	
Heavy atoms	1.21 ± 0.24
Backbone atoms	0.81 ± 0.24

NC2 forms higher order oligomers in solution, purified NC2 was subjected to size-exclusion chromatography (SEC). Under all concentrations tested (1–5 mg/mL in 20 m*M* sodium phosphate buffer, pH 7.0), NC2 eluted as one single peak (Fig. 2). The molecular weight of NC2 as calculated from multi-angle laser light scattering (MALLS) remained stable over this concentration range (average M_w 7.6 ± 0.3 kDa), indicating that NC2 is monomeric in solution up to 5 mg/mL under these conditions. ^{15}N-HSQC spectra recorded throughout the data acquisition period (over 1–2 weeks) showed little change in peak position, resolution and intensity suggesting the NMR sample is stable over time (including no change in the ratio of the major to minor conformers) and NC2 remains predominantly monomeric (Supporting Information Figure S1). However, it was observed that upon vigorous agitation NC2 solutions became white and turbid (Fig. 3A). After standing the agitated solution at room temperature, the white turbidity became concentrated at the meniscus, leaving the bulk solution clear. Examination of the vortexed NC2 solution by light microscopy revealed many air bubbles surrounded by a coating with distinct optical properties and the air bubbles remained stable for at least one day. This suggests that NC2 is surface active and is able to self-associate into a protein film at an air:water interface.

To further assess the surface activity of NC2 and its ability to reverse the wettability of hydrophobic surfaces, we compared the contact angles formed by water drops on octadecyltrichlorosilane (OTS)-coated silicon wafers and on an NC2 layer dried onto the same surface (Fig. 3B). Coating of the hydrophobic OTS-silicon wafer with NC2 reduces the contact angle of a water drop from 102.6 ± 1.4° to 48.5 ± 2.4°, showing that the presence of the NC2 film has greatly increased the wettability of the OTS-silicon wafer (Fig. 3C). The reduction in contact angle after NC2 coating is significantly larger than that observed with a coating composed of $EAS_{\Delta15}$, a modified form of the Class I hydrophobin EAS from *N. crassa* that has a truncated Cys3–Cys4 loop but retains wild type-like properties and rodlet-forming activity.[31] The $EAS_{\Delta15}$ form was used for this study because it has superior expression and purification properties to the wild type protein, has been well characterized and forms rodlets that are indistinguishable from WT EAS in terms of morphology and stability.[31,32] The $EAS_{\Delta15}$ coating only decreases the contact angle of a water drop to 69.2 ± 1.8°. It was also observed that both NC2 and $EAS_{\Delta15}$ protein drops on OTS-coated silicon wafers developed a trapezoid shape within 30 min of incubation (Fig. 3D). A protein film could be seen at the surface of the protein drops, resulting in the distorted drop shape. These observations demonstrate that NC2 layers can form at an air:aqueous-solution interface as well as on a hydrophobic surface from an aqueous solution.

NC2 assemblies are not amyloids

Unlike the rodlets formed by Class I hydrophobins, the polymeric form of NC2 that assembles at the air:-water interface does not bind the amyloid-specific dye Thioflavin T (ThT) and therefore does not have an amyloid-like substructure. Vigorous and extended

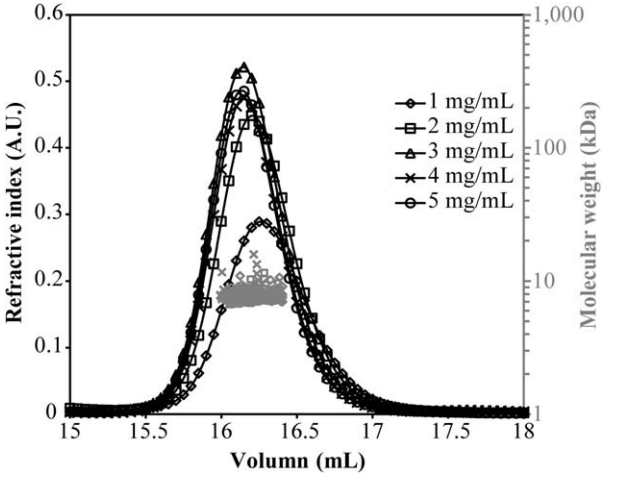

Figure 2
NC2 is monomeric in solution. SEC-MALLS profiles of NC2 from different loading concentrations. Protein elution was detected by the refractometer (solid lines, black symbols and left axis), and the molecular weight as calculated by MALLS is indicated with corresponding symbols (gray symbols and right axis). The average MW for NC2 determined over this concentration range by this method is 7.6 ± 0.3 kDa.

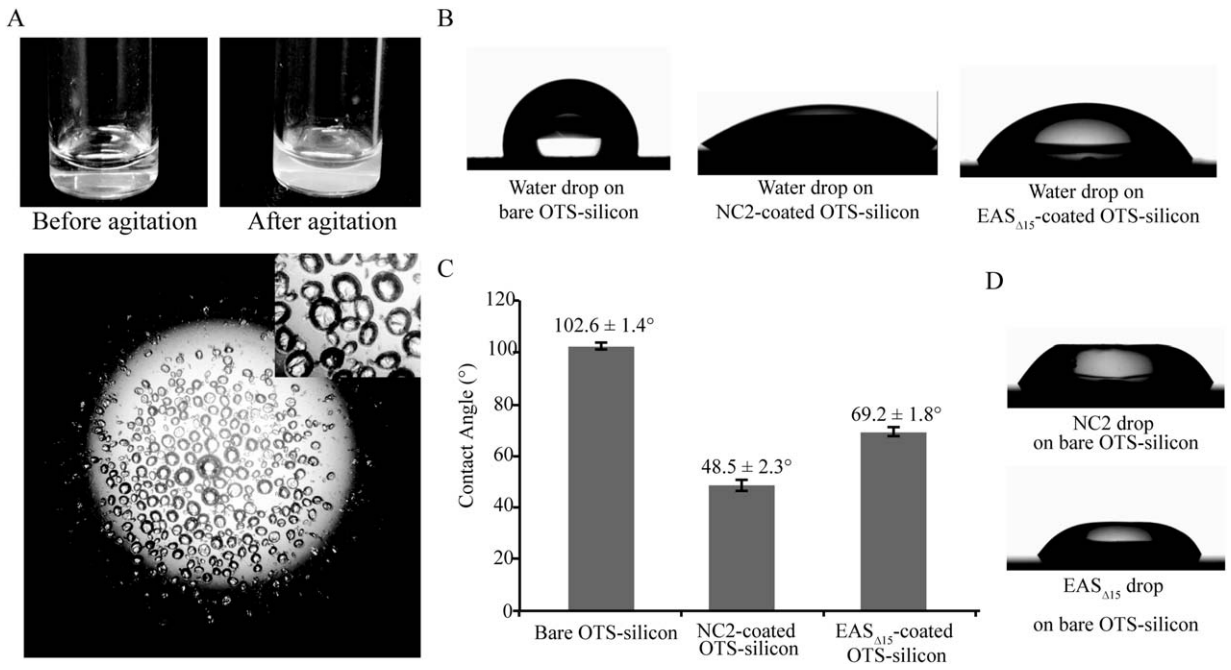

Figure 3

NC2 is highly surface active. **A**: Pictures of NC2 solution not subjected to agitation (top left) and the white and turbid NC2 solution after agitation for five minutes (top right), and an image taken on a light microscope of a drop of the NC2 solution that had been agitated (bottom). **B**: Pictures of water drop profile on bare, NC2, or EAS$_{\Delta15}$ coated OTS-silicon wafers. **C**: Corresponding water contact angles measured from water drops on bare, NC2, or EAS$_{\Delta15}$ coated OTS-silicon wafers. Errors bars are shown as one SD from the mean of three replicates. **D**: Pictures of drop profiles of NC2 or EAS$_{\Delta15}$ solution after incubation in air at room temperature for 30 min.

vortexing of an NC2 solution in the presence of ThT does not result in an increase of fluorescence signal (Fig. 4A), whereas the Class I hydrophobins EAS and EAS$_{\Delta15}$ rapidly form ThT-positive rodlets under the same conditions (Fig. 4B). Minor changes in the ThT emission spectra can be observed after agitation of the NC2 sample, however, they occur mainly at <450 nm and outside the ThT fluorescence emission band. These changes are likely to be due to scattering effects, since the solution of NC2 protein became turbid after agitation (Fig. 3A). The interface-driven self-assembly of NC2 is not accompanied by significant conformational changes, as FTIR spectra collected from monomeric and assembled NC2 samples display very similar profiles, with a maximum absorbance at 1640 cm^{-1} (Fig. 4C). This contrasts with the increase in β-sheet structural content observed upon rodlet assembly by the Class I hydrophobin EAS$_{\Delta15}$, which is consistent with formation of an amyloid structure.[33]

The NC2 monolayer is stabilized by hydrophobic interactions

The morphology and stability of the monolayer formed by NC2 was analyzed by atomic force microscopy (AFM). A very dilute protein solution was dried onto freshly cleaved highly oriented pyrolytic graphite (HOPG) substrate, a hydrophobic surface that is flat at the atomic level and suitable for AFM, and then washed with Milli-Q® water and imaged. The NC2 assembly exhibited a striking morphology (Fig. 5A). This morphology was observed in samples produced from three preparations of NC2. The layer formed by NC2 is 1.5- to 2-nm thick and consists of a network of protein molecules arranged into polygons. The repeating polygon units are around 30–90 nm in diameter, appear to be interconnected at five to six points and bear some resemblance to a published AFM image of HFBI.[34] In the HFBI images, the proteins are organized in repeating hexagonal units with a diameter of 20–30 nm^2, and the pattern is more regular and uniform than is observed for the NC2 polygon layer. However, the HFBI films were prepared by compression with a Langmuir trough, which laterally compacts the hydrophobin film and might have facilitated the more uniform arrangement. It is not known whether an uncompressed HFBI film will also display such a uniformly packed morphology.

There is great interest in using hydrophobins as biocompatible coatings in many biotechnology applications. While an extremely stable and robust hydrophobin layer is desirable for some applications, coatings which can be more readily depolymerized can also be advantageous, for example for solubilizing poorly water-soluble drugs for oral delivery.[35–37] Therefore, it is important to

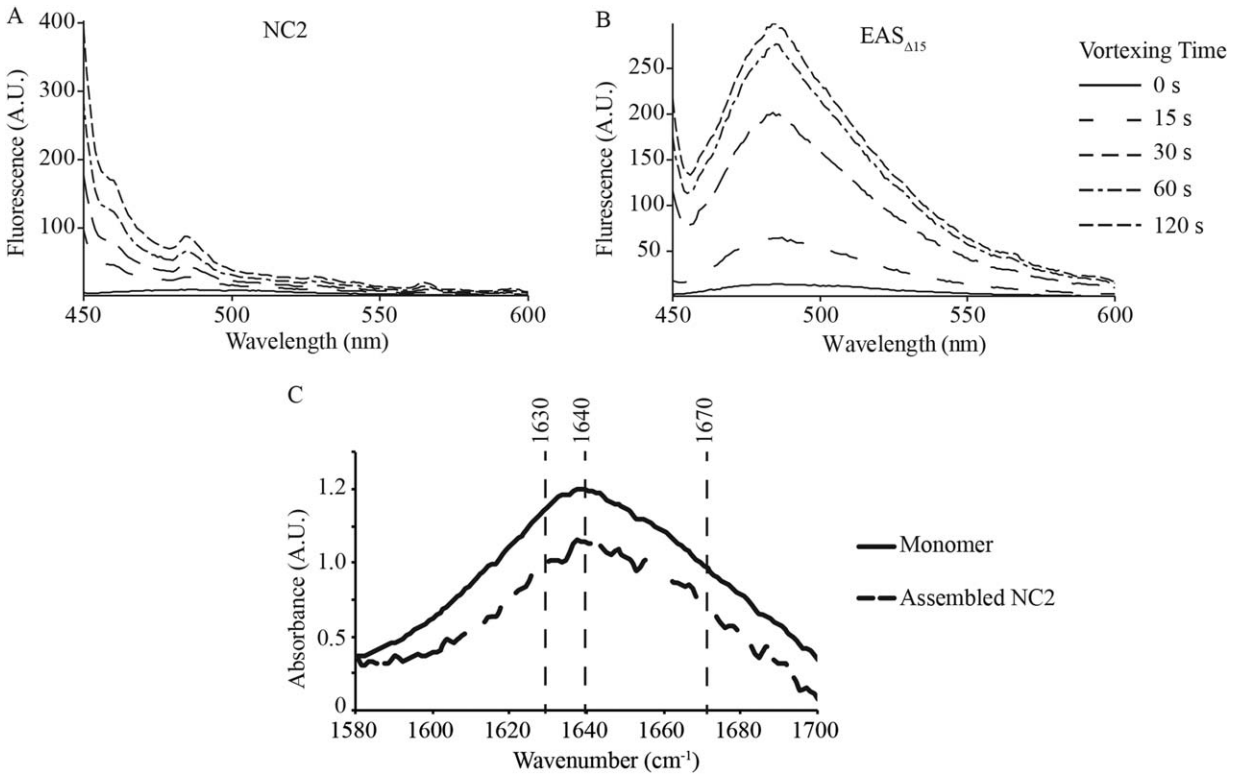

Figure 4

NC2 assemblies do not contain amyloid structure. ThT emission spectra of (**A**) NC2 and (**B**) EAS$_{\Delta 15}$ solutions before and after agitation for 15, 30, 60, and 120 s. C. FTIR spectra recorded on lyophilized monomer (solid line) and assembled NC2 (dotted line).

understand how stable the hydrophobin coatings are, under a variety of solution conditions. AFM was chosen to investigate the stability of NC2 monolayers, as this technique can simultaneously show whether the monolayer is stable toward a treatment and also reveal any alterations in the morphology of the monolayer if the protein layer has been disturbed.

NC2 monolayers were prepared as above and then incubated with 60% (v/v) ethanol, 3*M* NaOH, or 3*M* HCl at 25°C or 2% (v/v) SDS at 60°C for 5 min (Fig. 5B). These conditions were chosen as they have been widely reported as probes for the stability of Classes I and II hydrophobin assemblies.[20,38] After treatment, the surfaces were washed extensively with water to remove any solubilized and loosely bound protein, and then dried in air. The NC2 monolayer was dissolved upon incubation with 2% (v/v) hot SDS and 60% (v/v) ethanol. After treatment with hot SDS or ethanol, only small and scattered protein aggregates could be observed on the HOPG surface. This observed susceptibility to detergent and alcohol solutions is consistent with the classification of NC2 as a Class II hydrophobin, since similar results have been reported for other Class II hydrophobins.[20,38] The treatment with 3*M* NaOH and 3*M* HCl was observed to have a less destructive effect on NC2 monolayers, as more protein remained bound to the surface after treatment. Although the morphology of the monolayer was disturbed by the acid and base, the remaining protein layer displayed some level of organization and was not completely amorphous. While strong acidic and basic conditions would be expected to affect salt bridges and hydrogen bonds, treatment with ethanol and SDS would be expected to disrupt hydrophobic interactions. Our observations suggest that the NC2 monomers mainly interact with each other, and bind to the HOPG surface, via hydrophobic interactions. Therefore hydrophobic interactions are likely to be the key driving force behind Class II hydrophobin monolayer assembly and explain why these monolayers can generally be depolymerized by hydrophobic solvents and detergents that disrupt hydrophobic interactions. This is in contrast to what we have demonstrated for EAS rodlets, which are stable toward ethanol, SDS and basic treatments but which are disrupted by treatment with acidic conditions.[33] The EAS rodlets are known to be stabilized by intermolecular hydrogen bonding, which is disrupted by strongly acidic conditions and competition for hydrogen bonding between backbone carbonyl and amide groups.

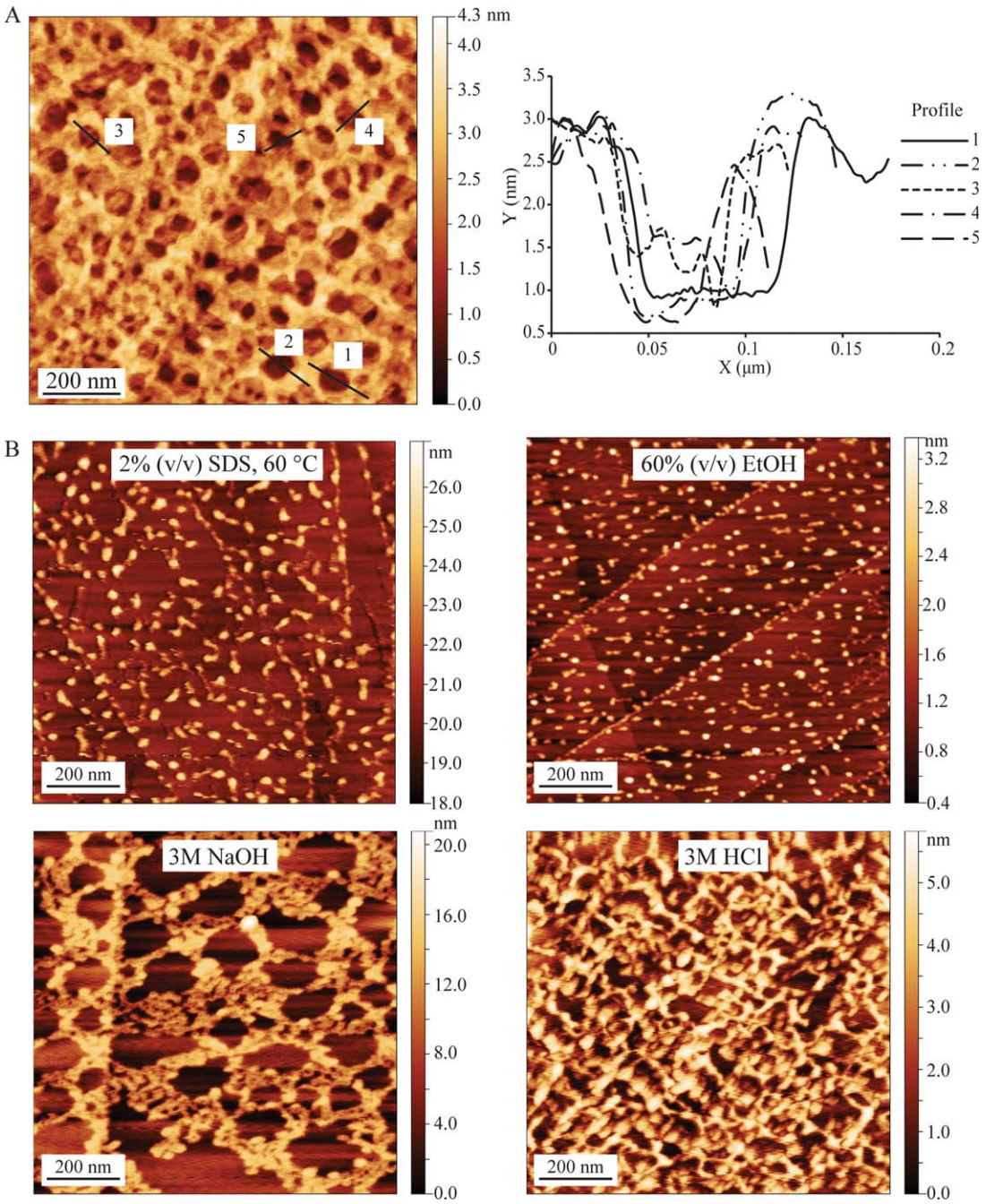

Figure 5

NC2 monolayers imaged by AFM. **A**: Left: topology image of NC2 monolayer formed on HOPG surface. Right: height profiles of the cross sections as marked in (A). **B**: NC2 monolayers after treatment with 2% (v/v) SDS at 60°C (middle left), 60% (v/v) EtOH (middle right), 3*M* NaOH (bottom left), or 3*M* HCl (bottom right). All treatments were performed at 25°C unless otherwise stated. [Color figure can be viewed in the online issue, which is available at wileyonlinelibrary.com.]

The solution structure of NC2

The structure of NC2 determined by solution NMR spectroscopy contains four antiparallel β-strands (named S1–S4), forming an open or half β-barrel, and one helix that lies on the surface of the barrel (Fig. 6A). In between the β-strands S1–S2 and S3–S4 are two loop regions (L1 and L2) that do not contain any regular secondary structure. Six of eight cysteine residues are located within or at the edge of the β-strands (Fig. 6B). Two disulfide bonds are formed between adjacent strands

(S1–S2 and S3–S4). The α-helix (Ala46–Ala54), which is located between S2 and S3, is linked to S1 by a disulfide bond. The last disulfide bond attaches Cys14 in the N-terminus to S3.

To study the backbone dynamics of NC2 in solution, in particular to ascertain whether the poorly defined N-terminus is also highly flexible, T_1 and T_2 relaxation time constants as well as heteronuclear NOE values were measured on each amide group. As shown in Figure 6(C), the N-terminus of the NC2 structure is highly dynamic. The remaining part of the protein chain is relatively rigid, even including those regions that do not contain any regular secondary structure elements, although a slightly greater level of flexibility is observed in the loops L1 and L2 than in the core as evidenced by a drop in the heteronuclear NOE values. The core of the NC2 structure appears to be tightly constrained by the network of four disulfide bonds.

Comparison of the NC2 structure with the structures of other hydrophobins identifies key structural features of these remarkable proteins and highlights distinctive features of each class. As can be seen from Figure 6(D), the conserved network of disulfide bonds stabilizes an open β-barrel structure upon which a range of structural elements are positioned. NC2, consistent with the Class II monolayer attributes, shares the peripheral α-helix between S2 and S3 that is observed in the structures of HFBI and HFBII. However, where in HFBI/II the β-strands are relatively long, bend inward and wrap around to close the barrel through interstrand hydrogen bonding, in NC2 the strands are shorter and the loops L1 and L2 do not interact with each other but instead extend from the surface of the molecule (Fig. 6E). The relaxation measurements on NC2 indicate these two loops are slightly more mobile than the remaining chain, however, no closed β-barrel state was found within the 20 lowest energy structures. When HFBI and HFBII were crystallized in the presence of detergent, a more extended L2 was observed in some of the molecules.[15] This suggests that the L2 loop has some structural plasticity in Class II hydrophobins and the closed barrel may be a conformation stabilized by crystal packing. Another observation that supports the view that the tip of L2 may adopt multiple conformations in solution is the assignment of a second set of chemical shifts corresponding to random coil structures for Leu68–Asp71 in NC2. Hence, the slightly shorter β-strands observed in NC2, and the more open state, are likely to reflect the dynamics of the molecule in solution.

Like other hydrophobins, NC2 contains a large proportion of hydrophobic residues. We have used the POPS algorithm[39] (http://mathbio.nimr.mrc.ac.uk/wiki/POPS) to calculate the hydrophobic and hydrophilic contributions to the total solvent accessible surface area of NC2 and compared these values to those obtained from the three-dimensional structures of other hydrophobins. The total solvent accessible surface area (SASA) of NC2 is 6198 Å^2, of which 64% is characterized as hydrophobic. This compares with a value of 61 and 60% for the Class I hydrophobins EAS and DewA. The calculated values for the hydrophobic SASAs of the monomers of HFBI and HFBII are 62 and 67%, respectively. As suggested by Hakanpää *et al.*, the rigidity of the hydrophobin core might play an important role in ensuring that the sizeable hydrophobic area remains exposed on the protein surface instead of being buried away from solvent molecules.[14] However, with HFBI and HFBII these patches become hidden within the dimer or tetramer interface, resulting in a decrease in overall hydrophobic SASA upon oligomerization to 48 and 33%, respectively. These values are closer to the 37% hydrophobic SASA calculated for ubiquitin, a highly soluble globular protein that is not surface active.

In addition to the overall hydrophobicity of the surface, hydrophobins also display distinct hydrophobic patches on the surface. We have used the Hotpatch algorithm[40] (http://hotpatch.mbi.ucla.edu/) to calculate the area of the largest discrete surface hydrophobic patch on HFBI and HFBII and find that the size of these are 783 and 891 Å^2, for the two proteins respectively. These represent 20 and 23% of the calculated total SASA and are close to the values of 19% reported by Hakanpää *et al.*[15] Using the Hotpatch algorithm we find that the areas of the largest discrete hydrophobic patches on NC2, EAS, and DewA are 693, 758, and 424 Å^2, respectively. By contrast, the largest single discrete exposed surface hydrophobic patch on ubiquitin has an area of only 268 Å^2.

In addition to the presence of large surface exposed hydrophobic regions, the particular distribution of the charged residues in NC2 is likely to contribute to the high surface activity of NC2. This hydrophobin contains nine charged residues, including two glutamate, four aspartate, and three arginine residues, of 80 residues. As can be seen in Figure 7(A), apart from Arg7 and Glu8, which are located in the poorly defined N-terminus before the first cysteine residue, the other charged residues all cluster on one side of the structure, leaving the opposite face free of charges. This distribution is similar to what is seen in the Class I hydrophobins EAS and DewA (Fig. 7A).

Structural and dynamic differences between Class II hydrophobins

Although the structure and assembly properties of NC2 confirm that it is a Class II hydrophobin, subtle features of the NC2 structure may explain its properties and the differences between NC2 and HFBI and HFBII. The N-terminal residues in NC2 are highly flexible whereas they are ordered in HFBI and HFBII. This is not unexpected given NC2 has 14 residues before the first cysteine residue whereas HFBI/II have only six and two,

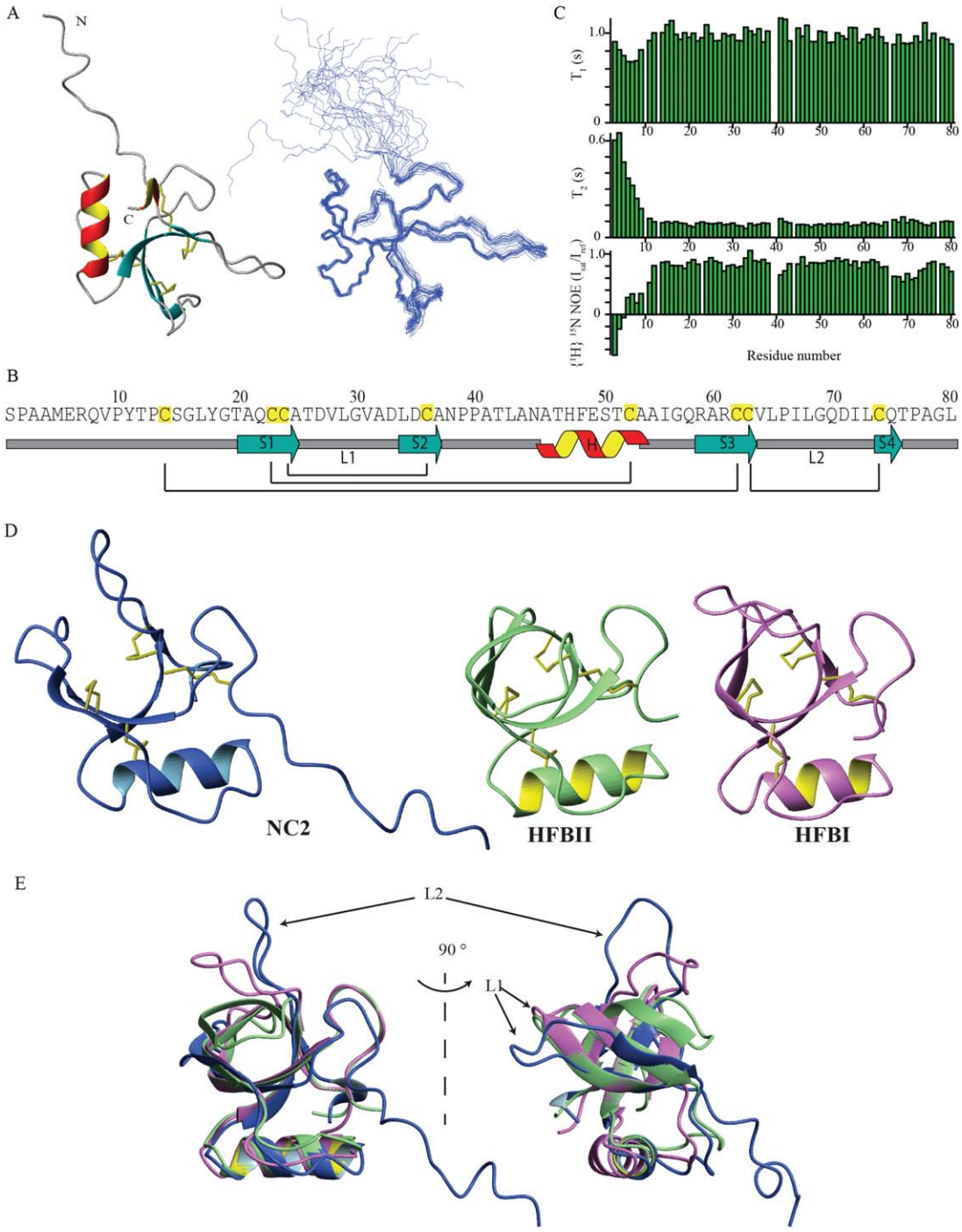

Figure 6

Solution structure and dynamics of NC2, and comparison of the Class II hydrophobin structures. **A**: Left: ribbon representation of the lowest energy structure of NC2. Secondary structures were calculated by MOLMOL[25] with disulfide bonds shown as yellow sticks. The termini are indicated with N and C. Right: 20 lowest energy models overlaid on the backbone atoms of the structured region (residues 11–80) with a RMSD of 0.81 Å. **B**: The secondary structure elements that are observed in the NC2 structure are indicated below the protein sequence. The four β-strands, the α-helix as well as the two loop regions are labeled. Cysteine residues are highlighted in yellow and disulfide bond connectivities are indicated with brackets below. Amino acid numbering is indicated above. **C**: Relaxation results are plotted across the protein sequence. A higher value indicates less molecular motion in the T_1 and ^{15}N-^{1}H NOE graphs, and more motion in the T_2 graph. **D**: Ribbon representations of the structures of NC2 (PDB 4aog), HFBII (PDB 2b97) and HFBI (PDB 2fz6) with disulfide bonds shown as yellow sticks. **E**: Overlay of the three Class II hydrophobin structures showing the different L1 and L2 conformations and the N-terminus. Secondary structure contents were calculated by MOLMOL.[25]

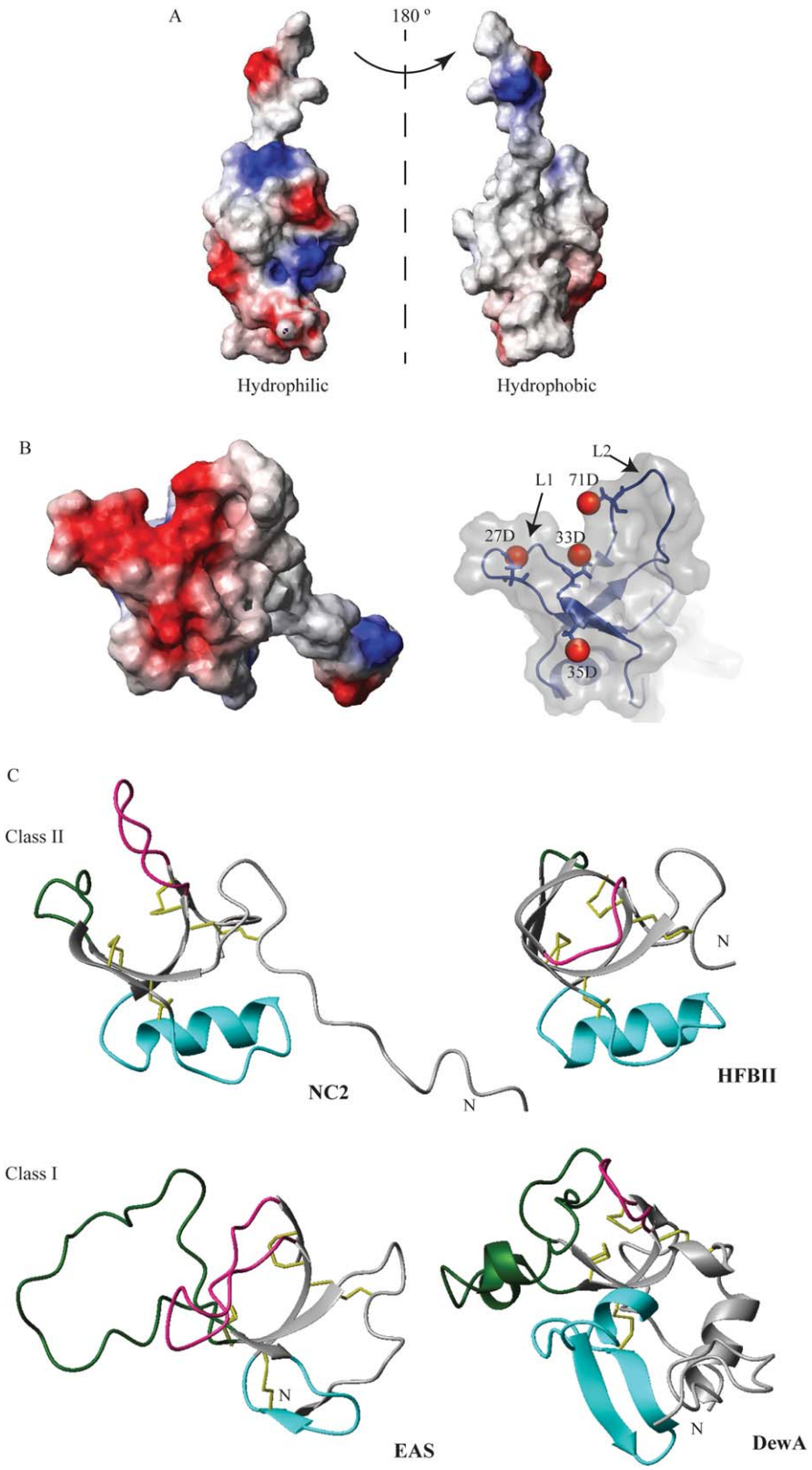

Figure 7

Electrostatic surface map of NC2 and comparison of hydropohobin structures. **A**: Plot of surface electrostatic potential of NC2 as calculated by MOLMOL[25] at pH 7.0, showing the hydrophilic (left) and hydrophobic (right) surface. Positively and negatively charges residues are colored in blue and red, respectively. **B**: View of the surface electrostatic potential of NC2 focused on the negatively charged area (red in the left image) and with the contributing OD_1 oxygen atoms of Asp residues shown as red spheres on the right. The surface representations of the NC2 structure were generated using PyMOL (Version 1.1r1). **C**: Comparison of structures from the two classes of hydrophobins. Ribbon representations of structures of Class II hydrophobins NC2 (PDB 4aog) and HFBII (PDB 2b97), and Class I hydrophobins EAS (PDB 2fmc) and DewA (PDB 2lsh). The L1 region is colored in dark green, L2 in pink, and the region between S2 and S3 is highlighted in cyan. Disulfide bonds are shown in yellow. Secondary structure elements are calculated by MOLMOL.[25] The positions of the N-termini are indicated.

respectively. In NC2 several regions contribute to the uncharged face of the protein, including residues near the N-terminus (Val9, Pro10, and Pro13), from L2 (Val64–Ile68), as well as Leu17, Ala21, Pro39–Ala41, and Leu43. In HFBI and II, the surface hydrophobic patch is mainly formed by residues from L1 and L2 (underlined in Fig. 1).[41] However, L1 in NC2 is negatively charged, containing four aspartate residues (Asp27, 33, 35, and 71, bold in Fig. 1), (Fig. 7B). Given the aspartate residues at position 27, 33, and 35 in NC2 are conserved in about half of the other Class II hydrophobins, it is likely the location and composition of the uncharged area of these other hydrophobins is more similar to that of NC2 and that variations exist between Class II hydrophobin members.

The differences observed in the location and makeup of the surface hydrophobic areas and in the N-terminus flexibility may explain the different solution behavior of Class II hydrophobins. The SEC-MALLS data clearly demonstrate that NC2 is monomeric up to 5 mg/mL whereas published data show that HFBI and HFBII form oligomers in solution and they have been crystallized as dimers and tetramers.[30] In these structures, the dimerization interface appears to be formed by the main hydrophobic patch from each monomer facing each other and being shielded from solvent and results in a large decrease in hydrophobic SASA, as discussed above.[14] This suggests that the hydrophobic interaction is the main driving force for the formation of oligomers in HFBI and HFBII, and may also explain why these two hydrophobins are soluble in water up to 100 mg/mL.[41] NC2 is only soluble up to a ~5 mg/mL and remains predominantly monomeric. As can be seen in Figure 6(A), NC2 has a highly disordered, flexible and relatively long N-terminus. It is likely that this interferes with dimerization of the protein. While a certain degree of structural plasticity is typically observed at the interaction surfaces between binding partners, a very high level of mobility, especially on both interaction surfaces as in the case of a symmetric dimer, is likely to be prohibitive of such interactions due to the high entropic cost involved. This flexibility may also explain why NC2 monolayers display a less regular morphology under AFM than is observed for compressed HFBI monolayers.[34]

Implications of the structural and dynamic features for hydrophobin monolayer assembly

Consistent with the much lower level of sequence conservation between Classes I and II hydrophobins, as well as within Class I hydrophobins, the structures of the three Class II hydrophobins are more similar to each other than to the Class I proteins (Fig. 7C). In general, Class II hydrophobin structures appear to be more ordered and compact than the Class I structures. Class II hydrophobins consist of the β-barrel, single tethered α-helix and relatively ordered loops L1 and L2. By contrast, the Class I hydrophobins EAS and DewA both contain large flexible loops which are only connected to the open β-barrel at each end and are therefore capable of major conformational change. Additionally, in EAS and DewA, the positions of large loop regions capable of major conformational change coincide with the location of an amyloidogenic sequence predicted by β-aggregation prediction algorithms, such as TANGO[42] and Waltz.[43] In the case of EAS, the amyloidogenic sequence has been confirmed experimentally using a mutagenesis screen and peptide assays.[32]

These structural and dynamic differences are consistent with the observation of a significant increase in β-sheet structure upon assembly of the Class I proteins EAS and DewA into a ThT-binding amyloid structure, whereas assembled NC2 does not have an amyloid structure and assembles into monolayers without undergoing large conformational changes. While rodlet formation by Class I hydrophobins occurs through conformational change that exposes amyloidogenic sequences for intermolecular association through β-sheet formation, Class II hydrophobins do not contain amyloidogenic sequences and have limited potential for conformational change between the first and last cysteine residues, hence do not form amyloid-based assemblies. The lack of requirement for major structural rearrangement is consistent with the more ordered and compact Class II monomer structures. The limited structural plasticity observed in Class II hydrophobins, for example in L2, may facilitate packing between neighboring units during monolayer formation or oligomerization in solution.

NC2—a new member of the Class II hydrophobin family

In summary, this work has demonstrated that NC2 from *N. crassa* is a Class II hydrophobin with high surface activity and the ability to form amphipathic monolayers that are stabilized by hydrophobic interactions and which are able to reverse the wettability of surfaces. Although no detailed studies of the biological functions of NC2 have been published, filamentous fungi typically express both Classes I and II hydrophobins, with individual hydrophobins exhibiting different spatial and temporal patterns and functions. Therefore, NC2 is likely to have a unique role in *N. crassa* biology that is distinct from that of the Class I hydrophobin EAS. Recently, Schmoll *et al.* reported that NC2 is significantly upregulated in *N. crassa* when either of the photoreceptors WC-1 or WC-2 is deleted. An NC2 knockout mutant shows an increase in cellulase activity, suggesting NC2 might be involved in reacting to the external environment and in plant host response.[18] NC2 displays a high sequence identity (67%) with MHP1, a Class II hydrophobin from

the rice blast fungus *Magnaporthe grisea* that has been implicated in host infection.[44] However, it must be noted that HFBI and HFBII have been shown to serve different purposes in *T. reesei*, despite sharing 63% of sequence identity, so further study to determine the precise role of NC2 is required.

Determination of the structure of NC2 indicates that the disulfide-constrained, open or half β-barrel is the core for both Classes I and II hydrophobins around which protein-specific elements are arrayed in different hydrophobins. In HFBI and HFBII the barrel is closed by extension of the strands but this is not a Class II-specific feature. This work also identifies intra- and interclass structural similarities and differences in the hydrophobin family and sheds light on the molecular basis for the different behavior of the two classes of hydrophobins and on the assembly mechanism of Class I rodlets and Class II monolayers.

ACKNOWLEDGMENTS

The authors thank Dr. N. Shepherd and Dr. B. Crossett for mass spectrometry at the Sydney University Proteome Research Unit, Dr. Alexey Kondyurin for access to the facilities for contact angle measurements, Drs. Chiara Neto and Manuel Ghezzi for access to the facility for AFM, and Dr. Stuart Thickett for the initial training in AFM operation.

REFERENCES

1. Wösten HA, van Wetter MA, Lugones LG, van der Mei HC, Busscher HJ, Wessels JG. How a fungus escapes the water to grow into the air. Curr Biol 1999;9:85–8.
2. Beever RE, Dempsey GP. Function of rodlets on the surface of fungal spores. Nature 1978;272:608–610.
3. Scherrer S, de Vries OMH, Dudler R, Wessels JGH, Honegger R. Interfacial self-assembly of fungal hydrophobins of the lichen-forming ascomycetes *Xanthoria parietina* and *X. ectaneoides*. Fungal Genet Biol 2000;30:81–93.
4. Scherrer S, Haisch A, Honegger R. Characterization and expression of XPH1, the hydrophobin gene of the lichen-forming ascomycete Xanthoria parietina. New Phytol 2002;154:175–184.
5. Trembley ML, Ringli C, Honegger R. Hydrophobins DGH1, DGH2, and DGH3 in the lichen-forming basidiomycete *Dictyonema glabratum*. Fungal Genet Biol 2002;35:247–259.
6. van Wetter MA, Wosten HA, Wessels JG. SC3 and SC4 hydrophobins have distinct roles in formation of aerial structures in dikaryons of Schizophyllum commune. Mol Microbiol 2000;36:201–210.
7. Lugones LG, Bosscher JS, Scholtmeyer K, de Vries OM, Wessels JG. An abundant hydrophobin (ABH1) forms hydrophobic rodlet layers in *Agaricus bisporus* fruiting bodies. Microbiology 1996;142 (Pt 5): 1321–1329.
8. Talbot NJ, Kershaw MJ, Wakley GE, de Vries O, Wessels J, Hamer JE. MPG1 encodes a fungal hydrophobin involved in surface interactions during infection-related development of *Magnaporthe grisea*. Plant Cell 1996;8:985–999.
9. Aimanianda V, Bayry J, Bozza S, Kniemeyer O, Perruccio K, Elluru SR, Clavaud C, Paris S, Brakhage AA, Kaveri SV, Romani L, Latgé JP. Surface hydrophobin prevents immune recognition of airborne fungal spores. Nature 2009;460:1117–1121.
10. Cox PW, Hooley P. Hydrophobins: new prospects for biotechnology. Fungal Biol Rev 2009;23:40–47.
11. Khalesi M, Venken T, Deckers S, Winterburn J, Shokribousjein Z, Gebruers K, Verachtert H, Delcour J, Martin P, Derdelinckx G. A novel method for hydrophobin extraction using CO_2 foam fractionation system. Ind Crops Prod 2013;43:372–377.
12. Ren Q, Kwan AH, Sunde M. Two forms—two faces, multiple states—multiple uses: properties and applications of the self-assembling fungal hydrophobins. Biopolymers 2013;100:601–612.
13. Wessels J. Developmental regulation of fungal cell-wall formation. Annu Rev Phytopathol 1994;32:413–437.
14. Hakanpää J, Paananen A, Askolin S, Nakari-Setälä T, Parkkinen T, Penttila M, Linder MB, Rouvinen J. Atomic resolution structure of the HFBII hydrophobin, a self-assembling amphiphile. J Biol Chem 2004;279:534–539.
15. Hakanpää J, Szilvay GR, Kaljunen H, Maksimainen M, Linder M, Rouvinen J. Two crystal structures of *Trichoderma reesei* hydrophobin HFBI–the structure of a protein amphiphile with and without detergent interaction. Protein Sci 2006;15:2129–2140.
16. Hakanpää J, Linder M, Popov A, Schmidt A, Rouvinen J. Hydrophobin HFBII in detail: ultrahigh-resolution structure at 0.75 A. Acta Crystallogr D Biol Crystallogr 2006;62:356–367.
17. Galagan JE, Calvo SE, Borkovich KA, Selker EU, Read ND, Jaffe D, FitzHugh W, Ma L-J, Smirnov S, Purcell S, Rehman B, Elkins T, Engels R, Wang S, Nielsen CB, Butler J, Endrizzi M, Qui D, Ianakiev P, Bell-Pedersen D, Nelson MA, Werner-Washburne M, Selitrennikoff CP, Kinsey JA, Braun EL, Zelter A, Schulte U, Kothe GO, Jedd G, Mewes W, Staben C, Marcotte E, Greenberg D, Roy A, Foley K, Naylor J, Stange-Thomann N, Barrett R, Gnerre S, Kamal M, Kamvysselis M, Mauceli E, Bielke C, Rudd S, Frishman D, Krystofova S, Rasmussen C, Metzenberg RL, Perkins DD, Kroken S, Cogoni C, Macino G, Catcheside D, Li W, Pratt RJ, Osmani SA, DeSouza CPC, Glass L, Orbach MJ, Berglund JA, Voelker R, Yarden O, Plamann M, Seiler S, Dunlap J, Radford A, Aramayo R, Natvig DO, Alex LA, Mannhaupt G, Ebbole DJ, Freitag M, Paulsen I, Sachs MS, Lander ES, Nusbaum C, Birren B. The genome sequence of the filamentous fungus *Neurospora crassa*. Nature 2003;422:859–868.
18. Schmoll M, Tian CG, Sun JP, Tisch D, Glass NL. Unravelling the molecular basis for light modulated cellulase gene expression—the role of photoreceptors in *Neurospora crassa*. BMC Genomics 2012;13:127.
19. Petersen TN, Brunak S, von Heijne G, Nielsen H. SignalP 4.0: discriminating signal peptides from transmembrane regions. Nat Meth 2011;8:785–786.
20. Kwan AH, Winefield RD, Sunde M, Matthews JM, Haverkamp RG, Templeton MD, Mackay JP. Structural basis for rodlet assembly in fungal hydrophobins. Proc Natl Acad Sci USA 2006;103:3621–3626.
21. Schubert M, Labudde D, Oschkinat H, Schmieder P. A software tool for the prediction of Xaa-Pro peptide bond conformations in proteins based on 13C chemical shift statistics. J Biomol NMR 2002;24: 149–154.
22. Vranken WF, Boucher W, Stevens TJ, Fogh RH, Pajon A, Llinas P, Ulrich EL, Markley JL, Ionides J, Laue ED. The CCPN data model for NMR spectroscopy: development of a software pipeline. Prot-Struct Funct Bioinform 2005;59:687–696.
23. Rieping W, Habeck M, Bardiaux B, Bernard A, Malliavin TE, Nilges M. ARIA2: automated NOE assignment and data integration in NMR structure calculation. Bioinformatics 2007;23:381–382.
24. Brunger AT, Adams PD, Clore GM, DeLano WL, Gros P, Grosse-Kunstleve RW, Jiang JS, Kuszewski J, Nilges M, Pannu NS, Read RJ, Rice LM, Simonson T, Warren GL. Crystallography & NMR system: a new software suite for macromolecular structure determination. Acta Crystallogr Sec D-Biol Crystallogr 1998;54:905–921.
25. Cheung M-S, Maguire ML, Stevens TJ, Broadhurst RW. DANGLE: a Bayesian inferential method for predicting protein backbone dihedral angles and secondary structure. J Magn Reson 2010;202:223–233.
26. Koradi R, Billeter M, Wuthrich K. MOLMOL: a program for display and analysis of macromolecular structures. J Mol Graph 1996;14:51.

27. Laskowski RA, Rullmann JAC, MacArthur MW, Kaptein R, Thornton JM. AQUA and PROCHECK-NMR: programs for checking the quality of protein structures solved by NMR. J Biomol NMR 1996;8:477–486.
28. Kisko K, Szilvay GR, Vainio U, Linder MB, Serimaa R. Interactions of hydrophobin proteins in solution studied by small-angle X-ray scattering. Biophys J 2008;94:198–206.
29. Szilvay GR, Nakari-Setälä, T, Linder MB. Behavior of *Trichoderma reesei* hydrophobins in solution: interactions, dynamics, and multimer formation. Biochemistry 2006;45:8590–8598.
30. Torkkeli M, Serimaa R, Ikkala O, Linder M. Aggregation and self-assembly of hydrophobins from *Trichoderma reesei*: low-resolution structural models. Biophys J 2002;83:2240–2247.
31. Kwan AH, Macindoe I, Vukasin PV, Morris VK, Kass I, Gupte R, Mark AE, Templeton MD, Mackay JP, Sunde M. The Cys3-Cys4 loop of the hydrophobin EAS is not required for rodlet formation and surface activity. J Mol Biol 2008;382:708–720.
32. Macindoe I, Kwan AH, Ren Q, Morris VK, Yang W, Mackay JP, Sunde M. Self-assembly of functional, amphipathic amyloid monolayers by the fungal hydrophobin EAS. Proc Natl Acad Sci USA 2012;109:E804–E811.
33. Yang W, Ren Q, Wu YN, Morris VK, Rey AA, Braet F, Kwan AH, Sunde M. Surface functionalization of carbon nanomaterials by self-assembling hydrophobin proteins. Biopolymers 2013;99:84–94.
34. Szilvay GR, Paananen A, Laurikainen K, Vuorimaa E, Lemmetyinen H, Peltonen J, Linder MB. Self-assembled hydrophobin protein films at the air-water interface: structural analysis and molecular engineering. Biochemistry 2007;46:2345–2354.
35. Zhao ZX, Wang HC, Qin X, Wang XS, Qiao MQ, Anzai J, Chen Q. Self-assembled film of hydrophobins on gold surfaces and its application to electrochemical biosensing. Colloids Surf B Biointerfaces 2009;71:102–106.
36. Bilewicz R, Witomski J, van der Heyden A, Tagu D, Palin B, Rogalska E. Modification of electrodes with self-assembled hydrophobin layers. J Phys Chem B 2001;105:9772–9777.
37. Sarparanta MP, Bimbo LM, Mäkilä EM, Salonen JJ, Laaksonen PH, Helariutta AM, Linder MB, Hirvonen JT, Laaksonen TJ, Santos HA, Airaksinen AJ. The mucoadhesive and gastroretentive properties of hydrophobin-coated porous silicon nanoparticle oral drug delivery systems. Biomaterials 2012;33:3353–3362.
38. Hou S, Li X, Li X, Feng XZ, Wang R, Wang C, Yu L, Qiao MQ. Surface modification using a novel type I hydrophobin HGFI. Anal Bioanal Chem 2009;394:783–789.
39. Cavallo L, Kleinjung J, Fraternali F. POPS: a fast algorithm for solvent accessible surface areas at atomic and residue level. Nucleic Acids Res 2003;31;3364–3366.
40. Pettit FK, Bare E, Tsai A, Bowie JU. HotPatch: a statistical approach to finding biologically relevant features on protein surfaces. J Mol Biol 2007;369:863–879.
41. Linder MB, Szilvay GR, Nakari-Setälä T, Penttila ME. Hydrophobins: the protein-amphiphiles of filamentous fungi. FEMS Microbiol Rev 2005;29:877–896.
42. Fernandez-Escamilla AM, Rousseau F, Schymkowitz J, Serrano L. Prediction of sequence-dependent and mutational effects on the aggregation of peptides and proteins. Nat Biotechnol 2004;22:1302–1306.
43. Maurer-Stroh S, Debulpaep M, Kuemmerer N, de la Paz ML, Martins IC, Reumers J, Morris KL, Copland A, Serpell L, Serrano L, Schymkowitz JW H, Rousseau F. Exploring the sequence determinants of amyloid structure using position-specific scoring matrices (vol. 7, p 237, 2010). Nat Methods 2010;7:855–855.
44. Kim S, Ahn IP, Rho HS, Lee YH. MHP1, a *Magnaporthe grisea* hydrophobin gene, is required for fungal development and plant colonization. Mol Microbiol 2005;57:1224–1237.